2011

Validation of the Atmospheric Chemistry Experiment by noncoincident MkIV balloon profiles

Voltaire A. Velazco
University of Wollongong, voltaire@uow.edu.au

G. Toon
California Institute of Technology

J.-F. Blavier
California Institute of Technology

A. Kleinbohl
California Institute of Technology

G. Manney
California Institute of Technology

See next page for additional authors

Validation of the Atmospheric Chemistry Experiment by noncoincident MkIV balloon profiles

Abstract

We have compared volume mixing ratio profiles of atmospheric trace gases measured by the Atmospheric Chemistry Experiment (ACE) version 2.2 and the MkIV solar occultation Fourier transform infrared spectrometers. These gases are H2O, O3, N2O, CO, CH4, HNO3, HF, HCl, OCS, ClONO2, HCN, CH3Cl, CF4, CCl2F2, CCl3F, COF2, CHF2Cl, and SF6. Due to the complete lack of close spatiotemporal coincidences between the ACE occultations and the MkIV balloon flights, we used potential temperatures and equivalent latitudes from analyzed meteorological fields to find comparable ACE and MkIV profiles. The results show excellent agreement for CH4, N2O, and other long-lived gases but slightly poorer agreement for shorter-lived species like CO, O3, and HCN. For example, in the upper troposphere (~400–650 K), maximum differences between MkIV and ACE are 2.4% for CH4, 1.7% for N2O, −12.4% for CO, −15.9% for O3, and −5.6% for HCN. In the lower stratosphere (~650–900 K), maximum MkIV-ACE differences are 7.6% for CH4, 14.1% for N2O, 7.3% for CO, −9.2% for O3, and 31.5% for HCN. Apart from a small vertical misregistration problem, the overall agreement between MkIV and ACE is very good.

Keywords

GeoQUEST

Publication Details

Velazco, V. A., Toon, G. C., Blavier, J. L., Kleinbohl, A., Manney, G. L., Daffer, W. H., Bernath, P. F., Walker, K. A. & Boone, C. (2011). Validation of the Atmospheric Chemistry Experiment by noncoincident MkIV balloon profiles. Journal of Geophysical Research D: Atmospheres, 116 (6), 1-17.

Authors

Voltaire A. Velazco, G. Toon, J.-F. Blavier, A. Kleinbohl, G. Manney, W. Daffer, P. Bernath, K. Walker, and C. Boone

Validation of the Atmospheric Chemistry Experiment by noncoincident MkIV balloon profiles

Voltaire A. Velazco,[1,2] Geoffrey C. Toon,[1] Jean-Francois L. Blavier,[1] Armin Kleinböhl,[1] Gloria L. Manney,[1] William H. Daffer,[1] Peter F. Bernath,[3] Kaley A. Walker,[4] and Chris Boone[5]

Received 19 August 2010; revised 14 December 2010; accepted 11 January 2011; published 25 March 2011.

[1] We have compared volume mixing ratio profiles of atmospheric trace gases measured by the Atmospheric Chemistry Experiment (ACE) version 2.2 and the MkIV solar occultation Fourier transform infrared spectrometers. These gases are H_2O, O_3, N_2O, CO, CH_4, HNO_3, HF, HCl, OCS, $ClONO_2$, HCN, CH_3Cl, CF_4, CCl_2F_2, CCl_3F, COF_2, CHF_2Cl, and SF_6. Due to the complete lack of close spatiotemporal coincidences between the ACE occultations and the MkIV balloon flights, we used potential temperatures and equivalent latitudes from analyzed meteorological fields to find comparable ACE and MkIV profiles. The results show excellent agreement for CH_4, N_2O, and other long-lived gases but slightly poorer agreement for shorter-lived species like CO, O_3, and HCN. For example, in the upper troposphere (~400–650 K), maximum differences between MkIV and ACE are 2.4% for CH_4, 1.7% for N_2O, −12.4% for CO, −15.9% for O_3, and −5.6% for HCN. In the lower stratosphere (~650–900 K), maximum MkIV-ACE differences are 7.6% for CH_4, 14.1% for N_2O, 7.3% for CO, −9.2% for O_3, and 31.5% for HCN. Apart from a small vertical misregistration problem, the overall agreement between MkIV and ACE is very good.

Citation: Velazco, V. A., G. C. Toon, J.-F. L. Blavier, A. Kleinböhl, G. L. Manney, W. H. Daffer, P. F. Bernath, K. A. Walker, and C. Boone (2011), Validation of the Atmospheric Chemistry Experiment by noncoincident MkIV balloon profiles, *J. Geophys. Res.*, *116*, D06306, doi:10.1029/2010JD014928.

1. Introduction

1.1. ACE-FTS

[2] The Atmospheric Chemistry Experiment (ACE) on board SCISAT-1 of the Canadian Space Agency is a solar occultation Fourier transform spectrometer (ACE-FTS). ACE was launched on 12 August 2003 into a 74° inclination, circular, 650 km altitude, Earth orbit, providing coverage that focuses on the polar regions. Coverage of the lower latitudes is relatively sparse (see Figure 1). Also, around the solstices, the spacecraft never enters the shadow of the earth and so there are no occultations. There are ~29 occultation events per day (~10,000/year), but not all of these could be telemetered back to Earth, especially in the first year of the ACE mission.

[3] ACE-FTS operates in the mid infrared range (750–4400 cm^{-1}) with a spectral resolution of 0.02 cm^{-1} (25 cm maximum optical path difference, OPD). It measures a large number of atmospheric trace gas species with a vertical resolution of 3–4 km from the cloud tops to about 150 km. A detailed description of the ACE mission is provided by *Bernath et al.* [2005]. A description of ACE data analysis methods is provided by *Boone et al.* [2005].

1.2. JPL MkIV Balloon-Borne Interferometer

[4] The JPL MkIV interferometer is a balloon-borne solar occultation FTIR spectrometer [*Toon*, 1991]. It was designed and built at the Jet Propulsion Laboratory, based on the ATMOS instrument [*Farmer*, 1987]. The MkIV covers the entire 650–5650 cm^{-1} region simultaneously at 0.01 cm^{-1} spectral resolution (56 cm maximum OPD). The JPL MkIV interferometer has performed 21 balloon flights since 1989. Flights are of 6–30 h duration depending on float winds. Each provides one or two occultation events covering altitudes from the cloud tops to the balloon (35–40 km) at 2–4 km vertical resolution. MkIV data analysis methods are summarized by *Sen et al.* [1996]. The MkIV has an established validation heritage that includes instruments on the UARS in the 1990s [*Russell et al.*, 1996], ILAS-1 [*Nakajima et al.*, 2006] and ILAS-2 [*Irie et al.*, 2006], in situ sensors on board NASA ER-2 aircraft

[1]Jet Propulsion Laboratory, California Institute of Technology, Pasadena, California, USA.
[2]Now at Institute of Environmental Physics, University of Bremen, Bremen, Germany.
[3]Department of Chemistry, University of York, York, UK.
[4]Department of Physics, University of Toronto, Toronto, Ontario, Canada.
[5]Department of Chemistry, University of Waterloo, Waterloo, Ontario, Canada.

0148-0227/11/2010JD014928

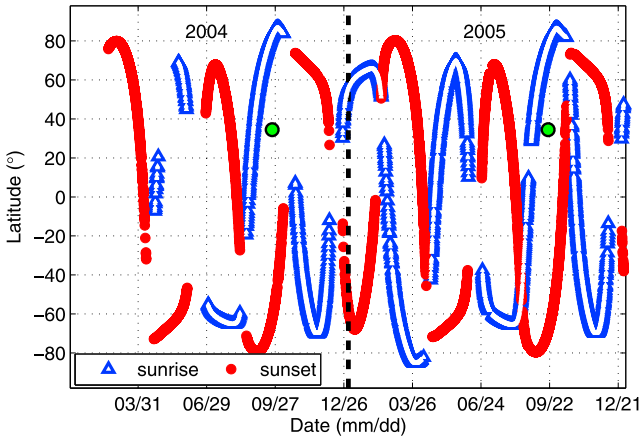

Figure 1. ACE occultation latitudes: sunset (red solid circles) /sunrise (blue triangles). Green ovals represent the fall turn-around periods at Fort Sumner (35°N). The lower density of points in 2004 was due to downlink limitations early in the mission.

[*Toon et al.*, 1999], POAM3 [*Randall et al.*, 2002] and MLS on AURA [*Froidevaux et al.*, 2006] (for a complete list, please refer to: http://mark4sun.jpl.nasa.gov/paper.html).

1.3. Review of Prior ACE Validation

[5] ACE products have been validated extensively using instruments from different platforms. As an example, *De Mazière et al.* [2008] provided a thorough validation of ACE CH_4 products using measurements from ground-based FTSs, the balloon-borne instrument SPIRALE [*Moreau et al.*, 2005] and satellite instruments MIPAS and HALOE. *Carleer et al.* [2008] augmented satellite comparisons of H_2O with LIDAR and frost point hygrometer data (see http://www.ace.uwaterloo.ca/publications.html for the validation papers). However, most of the validation efforts focused on comparisons with other satellite instruments or comparisons with instruments that use different techniques [see also *Walker et al.*, 2005]. There has so far been no ACE validation performed by another solar occultation FTS.

[6] The MkIV instrument is ideally suited instrument for ACE validation since it measures the same gases in the same spectral regions using the same technique (i.e., solar occultation spectrometry). However, to date, the MkIV balloon profiles have not been used much for ACE validation. This is because all the MkIV flights performed since ACE launched (2003) have been from Fort Sumner, New Mexico (35°N), in late September, which unfortunately falls in a gap in the ACE coverage (see Figure 1). The ACE occultations at this time are either at 80°N or 60°S and therefore far from 35°N. The closest ACE measurements at similar latitudes are 2–3 weeks later than those of MkIV and therefore fail any normal sort of a coincidence criterion. Therefore, directly comparing MkIV and ACE profiles must be done very carefully.

[7] The choice of the late September period for MkIV balloon flights is because this is when the stratospheric wind changes from Easterly to Westerly. During this so-called turn-around period, the light float winds make it possible to perform flights of up to 30 h duration with the balloon remaining within telemetry range. The late-September turnaround is preferred to the one in early May because it is more predictable [*Wunch et al.*, 2005] and because the surface winds are usually lighter.

2. Methods

[8] In this section, we describe a method of noncoincident validation using, as an example, CH_4 from the September 2005 MkIV flight. In this study, we used the ACE version 2.2 profiles with updates to O_3. We do not claim that this method is new. The benefit of using a Potential Vorticity/Potential Temperature (PV/Theta) coordinate system for assimilating/comparing data sets has been understood for years [e.g., *Lait et al.*, 2004; *Manney et al.*, 2001]. But to the best of our knowledge, this is the first time that this technique has been applied to the ACE or MkIV data sets. Alternative methods to validate noncoincident measurements exist; for example, *Hegglin et al.* [2008] used tracer-tracer correlations and vertical tracer profiles relative to tropopause height and showed that the latter method reduced geophysical noise in the UT/LS region (within 6 km of the tropopause). The MkIV profiles, however, extend up to 38 km altitude for many gases and so we did not want to restrict the comparison to the UT/LS altitudes only. Therefore, we present a different approach in this study.

[9] Figure 2 (top) shows a comparison of a single MkIV CH_4 profile (colored squares) with more than 30 ACE profiles acquired within 6° of latitude and 6 weeks of the MkIV profiles. There is a wide spread of ACE VMRs in the stratosphere. The ACE zonal mean (black dashes) agrees poorly (up to 20% differences) with the MkIV profile. Both the MkIV and ACE data in Figure 2 are color-coded by their Equivalent Latitude (EqL), calculated using the procedures described by *Manney et al.* [2007]. EqL is calculated from the potential vorticity (PV) field on isentropic surfaces; the EqL of a given PV contour is the latitude that would encompass between it and the pole the same area as is enclosed by the PV contour. Because PV on isentropic surfaces can be regarded as a tracer of atmospheric motions, different EqL values distinguish air with different origins. It can be seen that the MkIV observations match well the ACE observations of the same color/EqL. This suggests that a method of comparing MkIV and ACE observations on the basis of EqL and potential temperature (θ) would do much better than one based on true latitude and altitude.

[10] Therefore, a method of noncoincident validation was developed. For each MkIV observation at a certain potential temperature (θ_m) and equivalent latitude (EqL_m), we determined the corresponding ACE VMR by fitting a surface to the ensemble of ACE data as a function of θ and EqL and then performing interpolation on this surface to the exact location (θ_m, EqL_m) of the MkIV observation. More specifically, the ACE data are represented by the first-order Taylor expansion

$$Y(\theta_i, EqL_i) = Y_0 + \alpha(\theta_i - \theta_m) + \beta(EqL_i - EqL_m) \qquad (1)$$

in the immediate vicinity of a MkIV observation. The index i represents different ACE observations. The three unknowns,

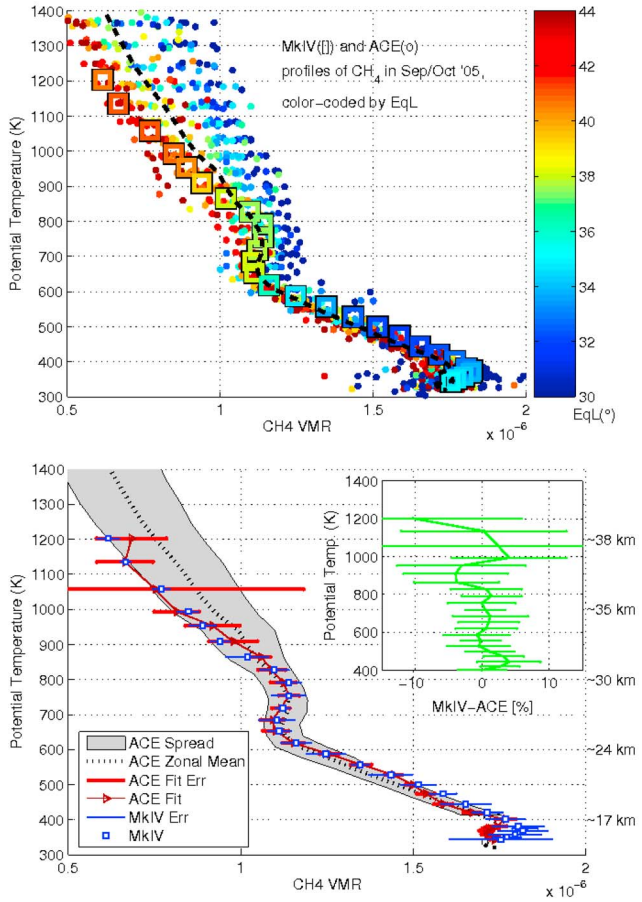

Figure 2. (top) Comparing the 2005 MkIV CH_4 profile (colored squares) with individual ACE profiles (colored dots) and with a zonal mean of the ACE results (black dashed line) acquired within 6° of latitude and 6 weeks of the MkIV. The color of the symbols represents the EqL. (bottom) By resampling the ACE data in θ/EqL space to match the MkIV observation locations, an ACE profile (red) that better matches the MkIV measurements (blue) is obtained. The gray shaded area shows the 1 σ spread in the ACE points. The percentage differences between ACE and MkIV VMR profiles are shown in the inset.

Y_0, α, and β were then obtained by minimizing the cost function

$$\chi^2 = \frac{\sum_i^n w_i \left[\frac{Y_i - Y_0 - \alpha(\theta_i - \theta_m) - \beta(EqL_i - EqL_m)}{\varepsilon_i}\right]^2}{\sum_i^n w_i} \quad (2)$$

where Y_i = CH_4 VMR for the ith ACE observation, ε_i = uncertainty in Y_i (the ACE-supplied uncertainty), Y_0, α, β = coefficients to be determined, and w_i = weights given for each ACE observation. Note that the $Y_0 = Y(\theta_m, EqL_m)$ is simply the value of the surface fitted to the ACE data at the coordinates of the MkIV observation, the quantity that we are seeking. The weights (w_i) depend on the closeness (in θ-EqL space) of the ACE and MkIV observation locations, and are given by

$$w_i = \frac{1}{1 + \left[\frac{\theta_i - \theta_m}{\Delta\theta}\right]^4 + \left[\frac{EqL_i - EqL_m}{\Delta EqL}\right]^4}. \quad (3)$$

[11] So the weights are ~1 for ACE measurements within $\Delta\theta$ and ΔEqL of the MkIV observation but fall off rapidly outside this range. The $\Delta\theta$ and ΔEqL criteria used here are 10 K and 4°, respectively. A $\Delta\theta$ of 10 K is chosen so that the weighting function's full width at half maximum (FWHM ~40 K) in the stratosphere would still overlap with the ACE vertical resolution. A ΔEqL of 4° means that the weighting function has a FWHM of ~8°. This roughly corresponds to the ensemble of equivalent latitudes that the MkIV samples during its flight (Figure 3). Without this weighting, the ACE points that are most distant from the MkIV observation would have the most leverage in determining the slope of the fitted surface. This weighting has been applied to all ACE data within the 6 week criteria. This time interval still falls within the stratospheric lifetime of CO, which is a suitable tracer. *Minschwaner et al.* [2010] showed that on average, the production lifetime of CO is 40–60 days throughout most of the sunlit stratosphere and mesosphere. The loss lifetime is about 10–60 days at mid-latitudes in September [*Minschwaner et al.*, 2010, Figure 9]. These numbers are consistent with the findings of *Rinsland et al.* [2000], where the CO lifetime at 800 K from 20°N to 35°N are reported to be 40 days. Moreover, the time scales for "nonconservative" changes in EqL and theta are primarily related to the diabatic descent rates. Their time scales are shortened at times and places where there is strong diabatic descent such as the fall/winter high-latitude regions, and more in the upper to middle stratosphere than lower down where descent rates are always lower. The MkIV and ACE measurements compared in this work are at a time (Sept) and place (35°N) where diabatic descent rates are small; hence the approximation of conservation of EqL and theta in an air mass over a period of even six weeks should be a good assumption. Note that all the Y values in all the equations above represent ACE VMRs. No use has been made yet of the MkIV VMRs–only the locations of the MkIV observations (θ_m, EqL_m) have been used so far.

[12] Y_0, α and β are obtained using the method of weighted least squares. This is done independently for each MkIV point. We could have fitted a single surface to the entire ensemble of ACE measurements, but this would have been a complicated and nonlinear function. Instead we have assumed that the ACE data are locally linear functions of θ and EqL in the vicinity ($\Delta\theta$, ΔEqL) of each MkIV data point, so the three-parameter least squares solution is straightforward, requiring no iteration. We have no interest in the retrieved values of α and β. We fit these parameters only to minimize potential biases in Y_0 arising from any asymmetry in the distribution of ACE measurements in θ-EqL space about the MkIV observations.

[13] Results of this method for the CH_4 case are shown in Figure 2 (bottom). The zonal mean (black dashed line) deviates from the MkIV measurements at altitudes above the 800 K theta level. However, the resampled (i.e., interpolated

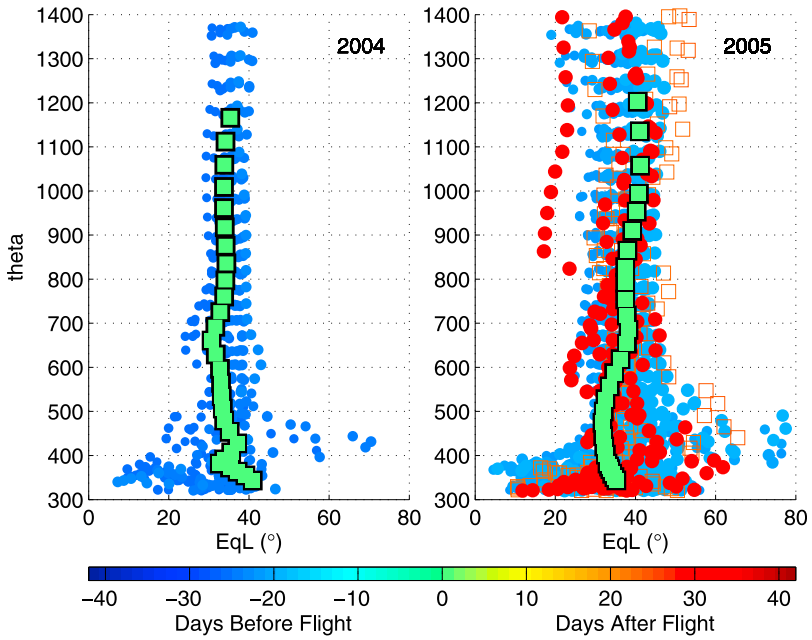

Figure 3. The θ, EqL coordinates of all the (left) 2004 and (right) 2005 MkIV and ACE points used in this study (only the 2005 points were used in Figure 2). ACE sunrise measurements are represented by circles, and sunsets are represented by open squares. The color coding represents the days before (blue) and after (red) the MkIV flight, which is represented by the solid green squares. Note that the MkIV observations fall within the range of the ACE observations at all altitudes. In 2004 the available ACE observations were solely sunrise data from before the MkIV flight. In 2005 a mix of sunrise/sunset data from before and after the MkIV flight was available.

in θ-EqL space) ACE VMRs ("ACE fit" red) agrees well with the MkIV profile (blue) and is within the MkIV error bars (blue). The percentage differences at each MkIV level are shown in the inset. The 1 σ errors in the % difference ($\sigma_{\%diff}$) between MkIV and the 2-D interpolated ACE profile (green lines) were calculated by taking into account the 1 σ error bars of the two VMR profiles, such that $\sigma_{\%diff} = (\sqrt{(\sigma^2_{MkIV} + \sigma^2_{ACE})}/VMR_{ave})*100\%$, where VMR_{ave} is the average VMR from ACE and MkIV.

[14] Figure 3 shows the EqL and θ of the MkIV observations (green) superimposed on those of the selected subset of ACE observations, i.e., taken within ±6 weeks and 6° of latitude of the MkIV measurements (no constraint was applied to the longitudes). Figure 3 shows that, in terms of EqL and θ, the MkIV measurements are well represented by the selected subset of ACE measurements; that is, there are no MkIV points outside the region of EqL and θ space occupied by ACE data. Although the ACE occultations during sunset (open squares) happened after the MkIV flight, they are very much evenly scattered in terms of equivalent latitude.

[15] A more complicated expression for the surface fitted to the ACE data was tried in which a fourth unknown γ was added representing the cross term between θ and EqL

$$Y(\theta_i, EqL_i) = Y_0 + \alpha(\theta_i - \theta_m) + \beta(EqL_i - EqL_m) + \gamma(\theta_i - \theta_m)(EqL_i - EqL_m). \quad (4)$$

This allows some curvature of the fitted surface. This equation is analogous to that used for bilinear interpolation. But we found no significant improvement in the quality of the fits using equation (4) compared with equation (2), indicating that the curvature of the surface fitting the ACE data within [$\Delta\theta$, ΔEqL] of the MkIV observations is small. We therefore used the simpler equation (2) for the analysis described below.

3. Results and Discussion

[16] We have applied the noncoincident validation method discussed above to 18 atmospheric gases and will provide a short discussion in this section. The plots of selected gases shown in Figures 4–21 are separated into two panels, with those on the left-hand side corresponding to the MkIV balloon flight in September 2004 and those on the right-hand side to September 2005. The plots and legends are the same as in Figure 2 (bottom). Table 1 summarizes the percentage biases for three atmospheric layers: 400–650 K, 650–900 K and 900 K up to the highest useable MkIV and ACE value (defined as positive VMR values with uncertainties less than 50%). The uncertainties of the biases in percent are given in the "Error" column.

[17] For most gases, the differences between MkIV and ACE for 2004 are slightly larger than for 2005. We attribute this to: (1) more ACE data used for the 2005 comparison, (2) the ACE data for 2004 were solely sunrise measurements and (3) the ACE measurements for 2004 were all taken 6 weeks before the MkIV flight (see Figure 3).

3.1. CH_4

[18] *De Mazière et al.* [2008] reported a CH_4 validation accuracy within 10% in the upper troposphere to lower

Table 1. Percentage Bias (MkIV Minus ACE) of Various Gases for Three Atmospheric Layers, 400–650 K, 650–900 K, and 900 K up to the Highest Useful ACE Value[a]

	Upper Troposphere (400–650 K)				Lower Stratosphere (650–900 K)				Midstratosphere (900 K to Useful ACE Value)			
	2004		2005		2004		2005		2004		2005	
Gas	Bias (%)	Error (%)	Bias (%)	Error (%)	Bias (%)	Error (%)	Bias (%)	Error (%)	Bias (%)	Error (%)	Bias (%)	Error (%)
H_2O	**−3.05**	6.07	1.33	9.03	**−1.44**	2.7	0.48	0.67	**−3.82**	1.94	2.6	2.75
O_3	**−15.89**	5.57	**−11.85**	7.65	**−9.16**	1.15	**−1.31**	1.03	**−9.68**	1.06	**−2.19**	1.12
N_2O	1.72	2.03	1.25	1.24	14.1	5.52	1.82	3.54	13.44	5.17	0.39	6.93
CO	**−6.32**	10.72	**−12.39**	4.26	7.26	5.31	5.97	2.46	15.35	11.34	16.76	8.45
CH_4	2.45	1.88	1.14	1.68	7.59	2.95	0.14	1.62	0.18	4.82	**−1.57**	4.57
HNO_3	**−4.34**	11.24	**−13.62**	8.35	5.97	7.01	**−2.21**	3.37	6.26	5.79	**−1.65**	3.32
HF	**−13.06**	11.29	**−7.59**	13.12	**−20.44**	6.14	**−10.82**	5.29	**−16.28**	4.74	**−7.91**	1.54
HCl	**−5.94**	7.31	**−3.65**	6.01	**−13.41**	4.85	**−5.77**	2.14	**−7.24**	3.43	**−6.62**	1.75
OCS	15.78	15.78	15.16	5.04	NaN	NaN	NaN	NaN	NaN	NaN	NaN	NaN
$ClONO_2$	**−22.01**	15.03	**−18.55**	19.44	**−14.44**	7.75	**−1.94**	9.15	**−49.05**	4.51	**−42.84**	10.32
HCN	**−5.57**	1.99	**−4.45**	3.81	31.52	26.95	**−1.11**	1.54	NaN	NaN	NaN	NaN
CH_3Cl	**−2.28**	14.49	**−10.19**	9.84	NaN	NaN	NaN	NaN	NaN	NaN	NaN	NaN
CF_4	9	5.12	10.44	3.87	**−0.66**	3.48	1.49	3	**−4.74**	2.93	**−3.45**	1.91
CCl_2F_2	11.64	2.6	10.31	3.75	12.84	1.17	6.97	7.7	NaN	NaN	NaN	NaN
CCl_3F	10.71	4.08	12.31	4.84	NaN	NaN	NaN	NaN	NaN	NaN	NaN	NaN
COF_2	**−3.59**	3.56	**−0.3**	8.16	3.55	10.5	6.99	5.9	NaN	NaN	NaN	NaN
CHF_2Cl	**−5.46**	13.34	**−1.4**	7.13	NaN	NaN	NaN	NaN	NaN	NaN	NaN	NaN
SF_6	**−2.30**[b]	17.6	**−1.94**[b]	21.40	NaN	NaN	NaN	NaN	NaN	NaN	NaN	NaN

[a]Values with higher ACE bias are boldface. NaN means that there are either no MkIV measurements or there are no useable ACE measurements for that region.
[b]SF_6 "Upper Troposphere" values are calculated at 350–550 K.

stratosphere and within 25% in the mid and higher stratosphere to the lower mesosphere. With our noncoincident method, we show an agreement better than 5% between ACE and MkIV from the upper troposphere to the mid-stratosphere and within 10% in the mid to upper stratosphere (Figure 2, inset, and Figure 4) for CH_4 in 2005.

3.2. H_2O

[19] H_2O is difficult to compare in the upper troposphere. First it can condense and is therefore short-lived and not a conserved tracer, especially near the tropical tropopause layer or TTL [*Notholt et al.*, 2010; *Steinwagner et al.*,

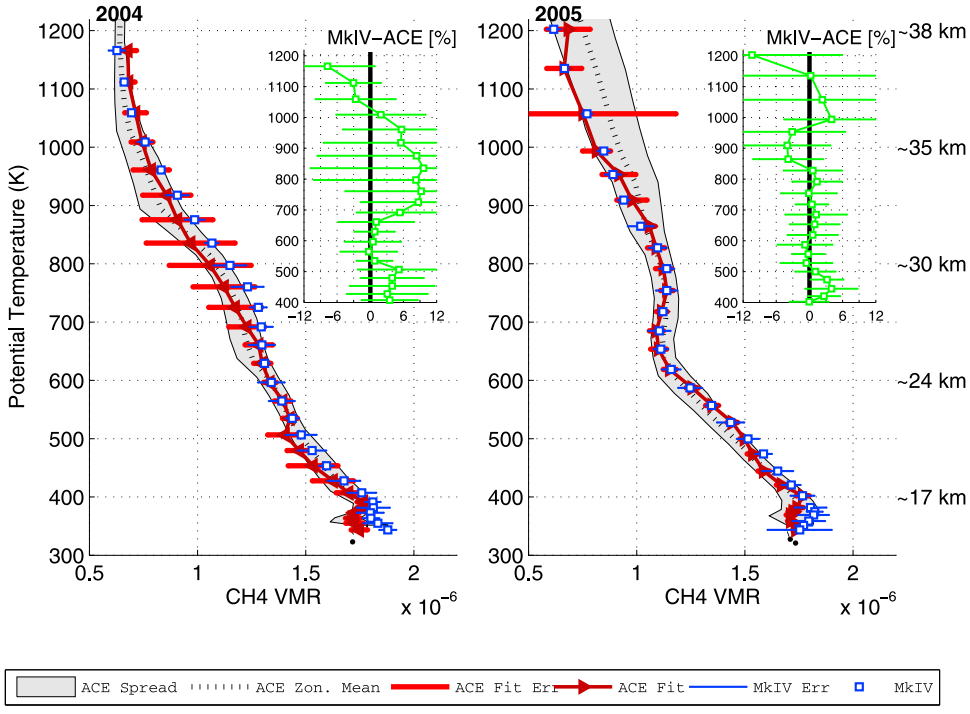

Figure 4. MkIV and ACE CH_4 comparisons with ACE data resampled in θ/EqL space (ACE fit, red lines) to match the locations of the MkIV measurements (blue squares). The gray shaded area shows the 1 σ spread in the ACE points. The percentage differences between ACE and MkIV VMR profiles are shown in the insets.

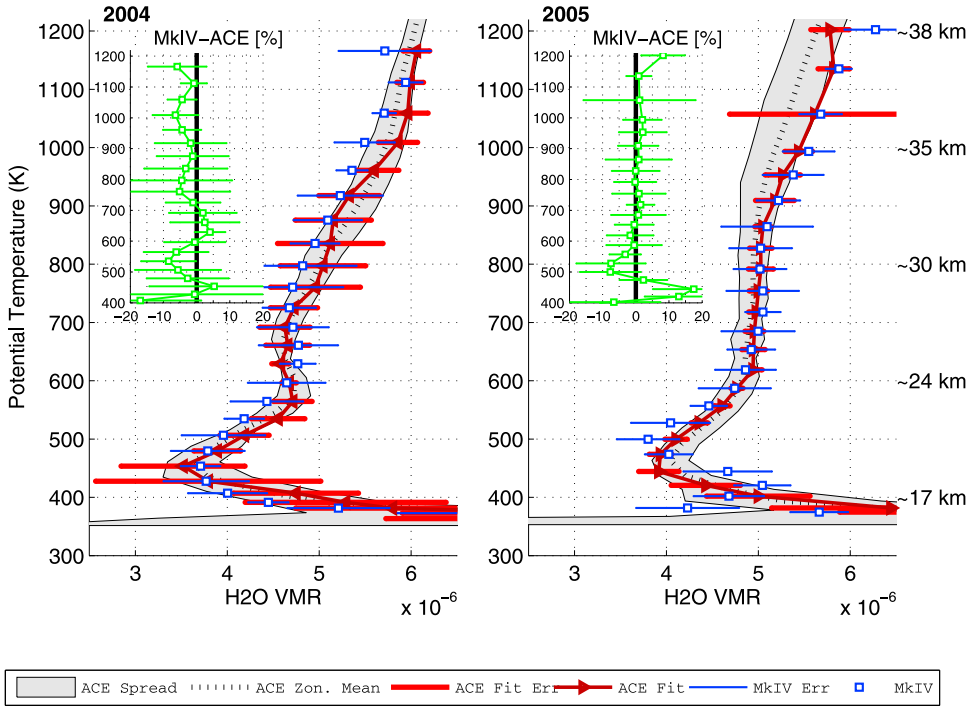

Figure 5. MkIV and ACE H_2O comparisons. Details as for Figure 4.

2010]. Second, there are large vertical gradients in H_2O which cause any intercomparison to be susceptible to vertical misregistration (error in altitude) of the data sets and to differences in vertical resolution (especially at the hygropause). So it should be no surprise to see MkIV/ACE differences of up to 20% below the hygropause (Figure 5). In the stratosphere, where H_2O is much longer lived and has much smaller vertical gradients, the agreement is much

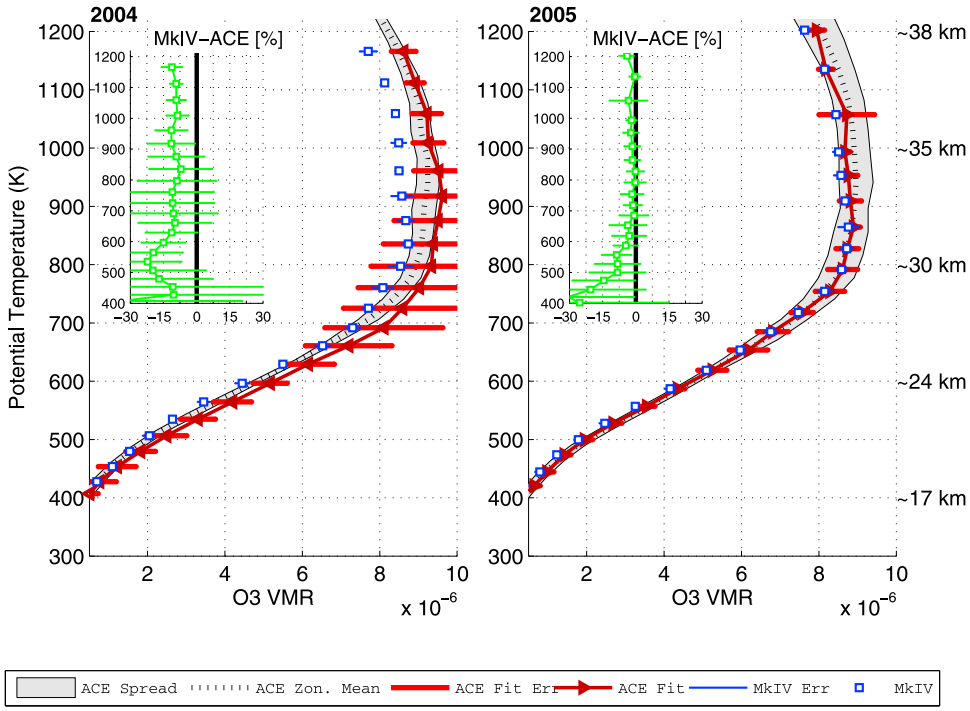

Figure 6. MkIV and ACE O_3 comparisons. Details as for Figure 4.

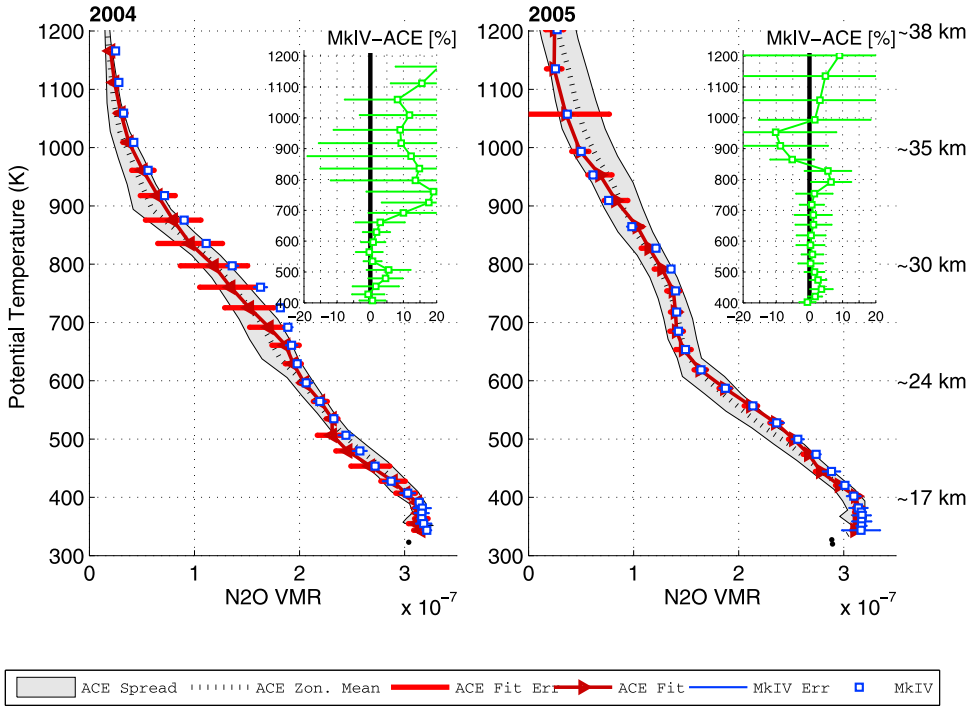

Figure 7. MkIV and ACE N_2O comparisons. Details as for Figure 4.

better with differences generally <5%. *Carleer et al.* [2008] compared ACE H_2O data with SAGE II, HALOE, POAM III, MIPAS and Odin SMR. They found that the difference between ACE H_2O profiles and that of the other instruments were about ±20% in the upper troposphere and better in the stratosphere.

3.3. O_3

[20] *Dupuy et al.* [2009] presented an extensive bias determination analysis of ozone observations from the ACE satellite instruments (FTS, MAESTRO). They compared the Ozone version 2.2 updated products with coincident observations from nearly 20 satellite, airborne, balloon-borne and ground-based instruments. MkIV data were not included in the comparison, probably due to the strict coincidence criteria the MkIV data would have not fulfilled during the comparison period (2004–2006). *Dupuy et al.* [2009] stated that the ACE-FTS version 2.2 O_3 updated products report more O_3 than most correlative measurements from the upper troposphere to the lower mesosphere. At altitude levels from 16 km to 44 km, the average values of the mean relative differences are nearly all within +1% to +8%. These values are consistent with the O_3 comparisons presented here (Figure 6). Above 600 K (~24 km), MkIV and ACE O_3 have differences ranging from about −1% to −10%, with better agreement for 2005, probably due to more ACE data. The ACE O_3 is consistently larger than the MkIV O_3 values, consistent with the observations presented by *Dupuy et al.* [2009].

3.4. N_2O

[21] ACE-FTS N_2O measurements have been validated by *Strong et al.* [2008] using profiles from satellite measurements (SMR, MLS, MIPAS), aircraft (ASUR), balloon (SPIRALE, FIRS-2) and partial columns from ground-based FTIR spectrometers. Satellite comparisons at 6 km to 30 km yielded a mean absolute difference of ±15%. *Strong et al.* [2008] also showed that ACE-FTS measurements are consistently smaller than the SPIRALE balloon-borne measurements between 17 km to 24 km, with relative differences of up to 19%. ACE-FTS also had a low bias relative to the balloon-borne measurements of FIRS-2 between 11 km to 13 km. Below 20 km, *Strong et al.* [2008] showed that the relative differences between ACE and SPIRALE measurements range from −6% to +17%.

[22] Comparisons with the MkIV measurements in this study (Figure 7) show some consistency with the results of *Strong et al.* [2008]. Overall, the agreement here is very good up to about 27 km, above that, MkIV measurements were higher than ACE in 2004 and lower than ACE in 2005. In 2004, the differences from this study are within 10% below ~27 km and within 20% below ~38 km for 2004. For 2005, the relative differences are within 10% or better than 4% at ~17 km to about 27 km. The comparison for the 2005 flight was better because ACE measurements for 2004 were taken 6 weeks after the MkIV flight. Although the MkIV equivalent latitude (*EqL*) values fall within the ACE *EqL*s, MkIV VMRs at altitudes of 700 K to 1100 K are at the edge of the ACE VMR distribution. This probably led to the relatively larger differences.

3.5. HCl, HF, $ClONO_2$, COF_2, and HNO_3

[23] Photolysis of man-made chlorofluorocarbons (CFC) in the stratosphere leads to the release of chlorine and fluorine atoms. This results in the formation of reservoir gases like HF, HCl, COF_2 and $ClONO_2$. These molecules

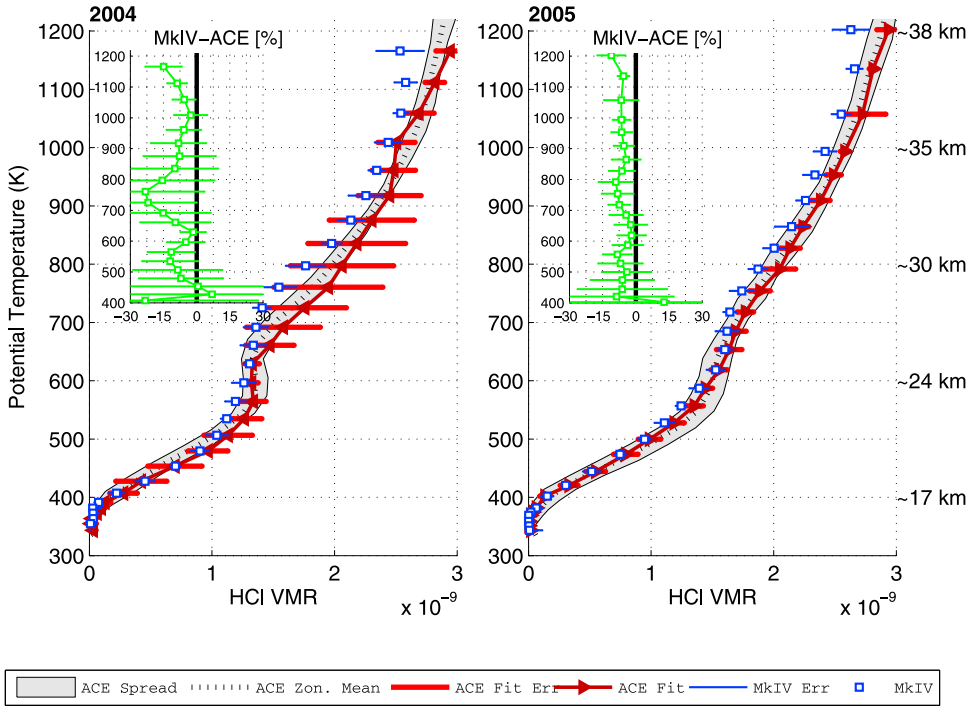

Figure 8. MkIV and ACE HCl comparisons. Details as for Figure 4.

have VMR profiles that increase with altitude in the lower and middle stratosphere. Their long lifetimes should also mean that ACE and MkIV profiles would agree better compared to profiles of gases that have shorter lifetimes. However, we see a strong negative MkIV-ACE bias for these gases in contrast to positive MkIV-ACE biases for gases that decrease in altitude, indicating vertical shifts in the retrieved profile.

[24] *Mahieu et al.* [2008] compared ACE-FTS measurements of HCl and HF with MkIV profiles taken over Fort Sumner during the 2003, 2004 and 2005 campaigns. Due to the absence of direct coincidences between ACE and MkIV, *Mahieu et al.* [2008] used zonal means from 90 ACE profiles over a latitude bin of ±5° width centered near Fort Sumner, between August and October in 2004, 2005 and 2006. They showed that above 20 km, ACE and MkIV HCl profiles are in good agreement (to better than ±7%) but differences become extremely large below 17 km. ACE also measured systematically higher HCl than FIRS-2 (20% to 60%) at 12 to 31 km for the Arctic comparison done by *Mahieu et al.* [2008]. However, they stated that the large discrepancies may have been influenced by the presence of polar stratospheric clouds (PSCs). In this comparison, ACE also shows consistently larger HCl values than the MkIV (Figure 8). For 2005, the relative differences range from approximately 0% to −10%. For 2004, most of the relative differences are within 0% to 10% as well, except for the region around 700 K (between 24 and 30 km) where ACE measures up to 20% more HCl than MkIV. In this altitude region, a "fold" in the profile can also be observed. It is more prominent in the ACE profile's zonal mean compared to the MkIV and the "ACE Fit" profile.

[25] Comparisons with HF zonal means from ACE with MkIV done by *Mahieu et al.* [2008] reported relative differences of about 10% above 19 km, with ACE profiles biased high. The same bias was shown by *Mahieu et al.* [2008] for comparisons with FIRS-2 and HALOE HF profiles. These findings are consistent with the results shown here, with ACE HF always larger in values (up to 30%) compared to MkIV above 500 K (Figure 9).

[26] *Wolff et al.* [2008] compared ACE and MIPAS $ClONO_2$ profiles. In their results, ACE reported smaller values (<5%) than MIPAS at nearly all altitudes and above 27 km, the differences increase to around 30%. In contrast, we observe here that below the $ClONO_2$ peak, ACE consistently reported more $ClONO_2$ than MkIV (Figure 10). This bias is consistent with the bias found for the HF and HCl comparisons with MkIV.

[27] The COF_2 comparisons in this work show a consistently higher ACE bias below 24 km only for 2005 (Figure 11). For COF2 (and several other weakly absorbing gases), the Version 2.2 ACE profiles extend only up to $\theta = 850$ K. Above this level, the gray shaded band represents the scaled ACE a priori profile, not a retrieval.

[28] HNO_3 validation done by *Wolff et al.* [2008] showed that ACE HNO_3 VMR profiles in the Arctic are typically larger (28%) than SPIRALE VMRs. ACE and FIRS-2 relative differences oscillate between −55% to +50% and are typically 20%. However, they reported that SPIRALE and FIRS-2 were affected by PSC and may have seen local denitrification. Our comparisons here show that MkIV and ACE HNO_3 differences oscillate between −20% and 20% above 500 K, with differences reaching 40% below 500 K (Figure 12). For 2004, ACE measures distinguishably less HNO_3 at the peak of the profile around 600 K (~24 km).

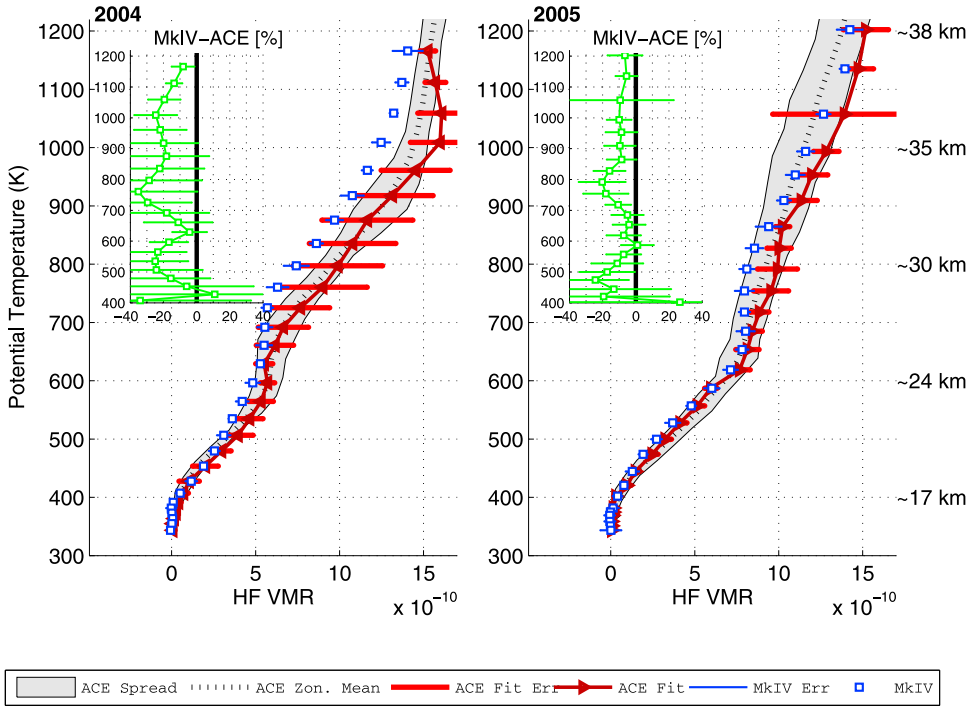

Figure 9. MkIV and ACE HF comparisons. Details as for Figure 4.

3.6. CFC-11 (CCl_3F) and CFC-12 (CCl_2F_2)

[29] *Mahieu et al.* [2008] compared CFC-11 from ACE with FIRS-2 measurements and found that ACE measures slightly lower (10%) CFC-11 from 12 km to 16 km. They reported the same scenario when they used ACE zonal mean profiles compared to MkIV profiles above 12 km measured in Fort Sumner. From the technique we used in this study, the resulting differences are better than 20% between ACE

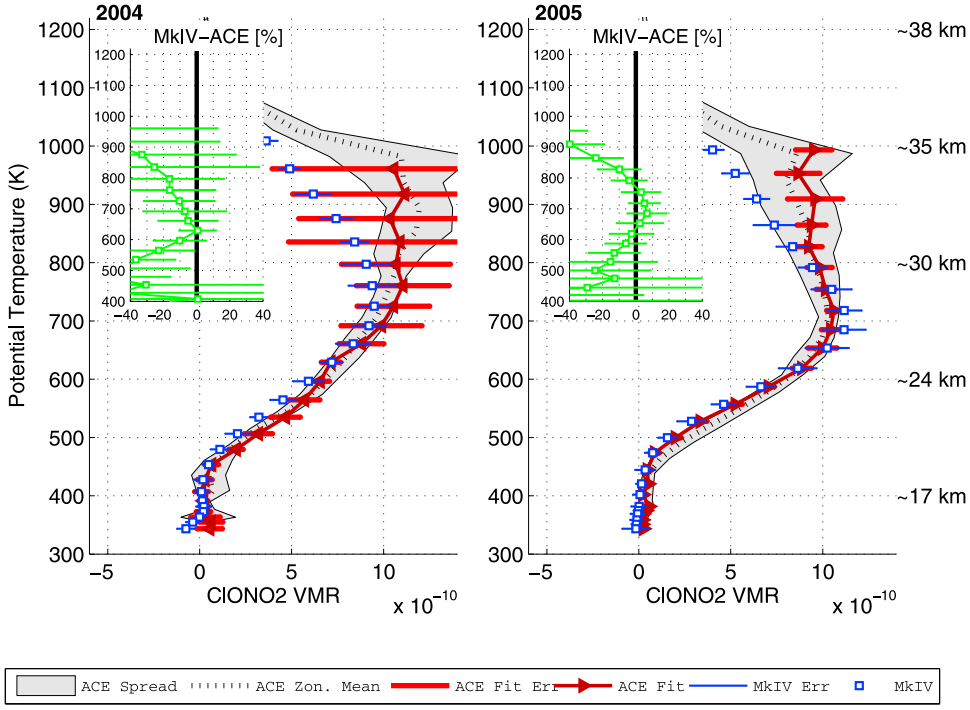

Figure 10. MkIV and ACE $ClONO_2$ comparisons. Details as for Figure 4.

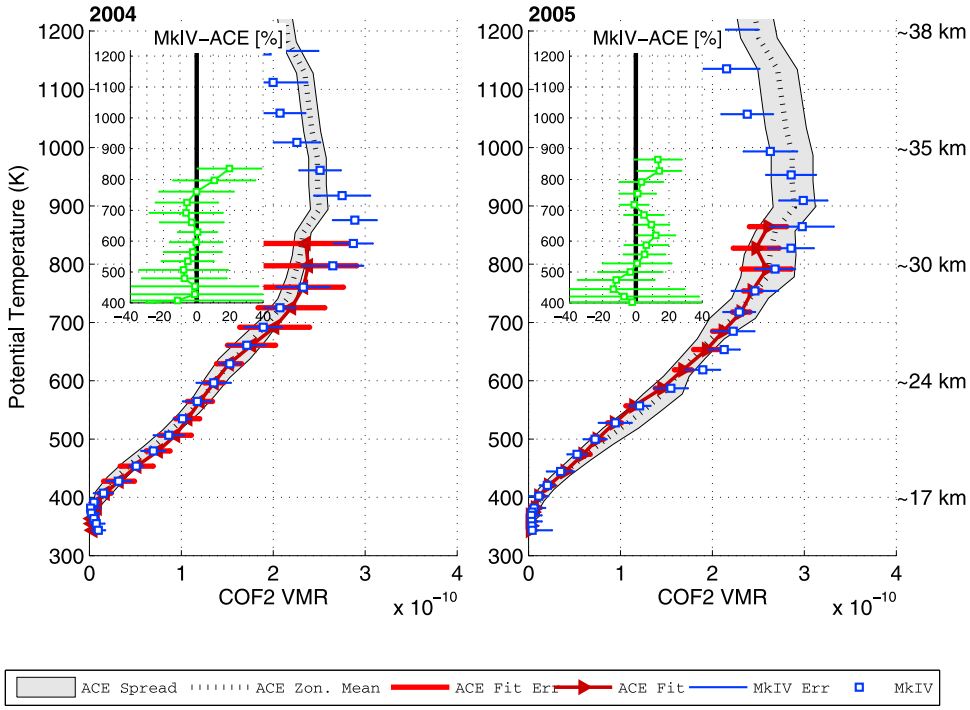

Figure 11. MkIV and ACE COF_2 comparisons. Details as for Figure 4.

and noncoincident MkIV profiles at ~17 km to 24 km, with ACE systematically lower than MkIV, similar to the *Mahieu et al.* [2008] comparisons. For CFC-12 comparisons with FIRS-2, *Mahieu et al.* [2008] found similar results with their comparisons for CFC-11, yielding maximum differences on the order of 10% (ACE biased low). We also find the same ACE bias in this study (Figures 13 and 14).

3.7. HCN

[30] HCN is mostly a product of incomplete combustion from biomass burning. It has a lifetime of more than

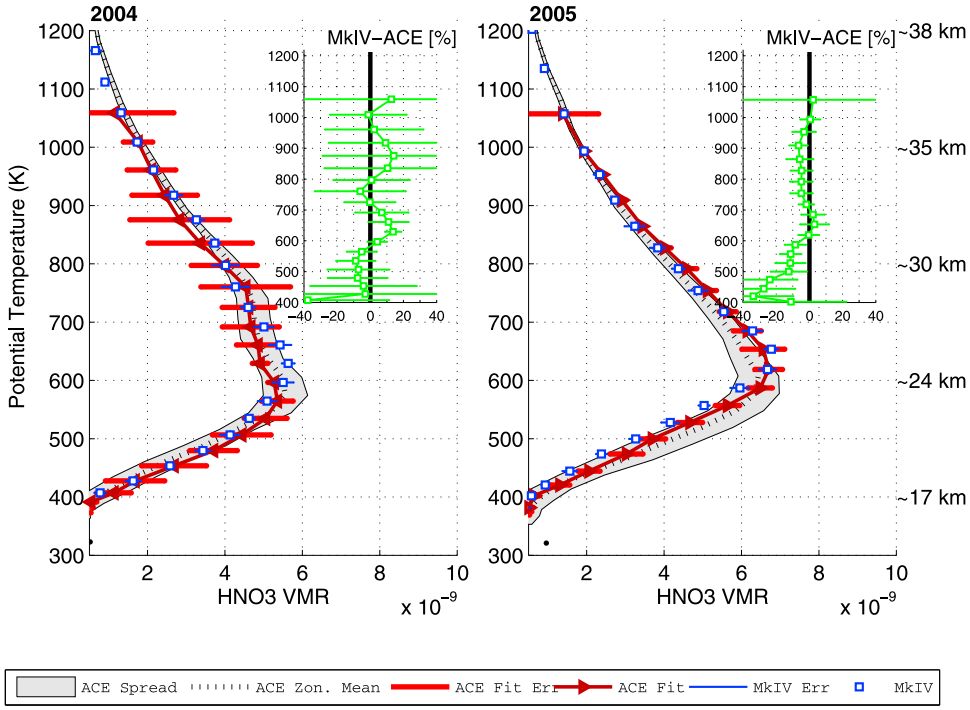

Figure 12. MkIV and ACE HNO_3 comparisons. Details as for Figure 4.

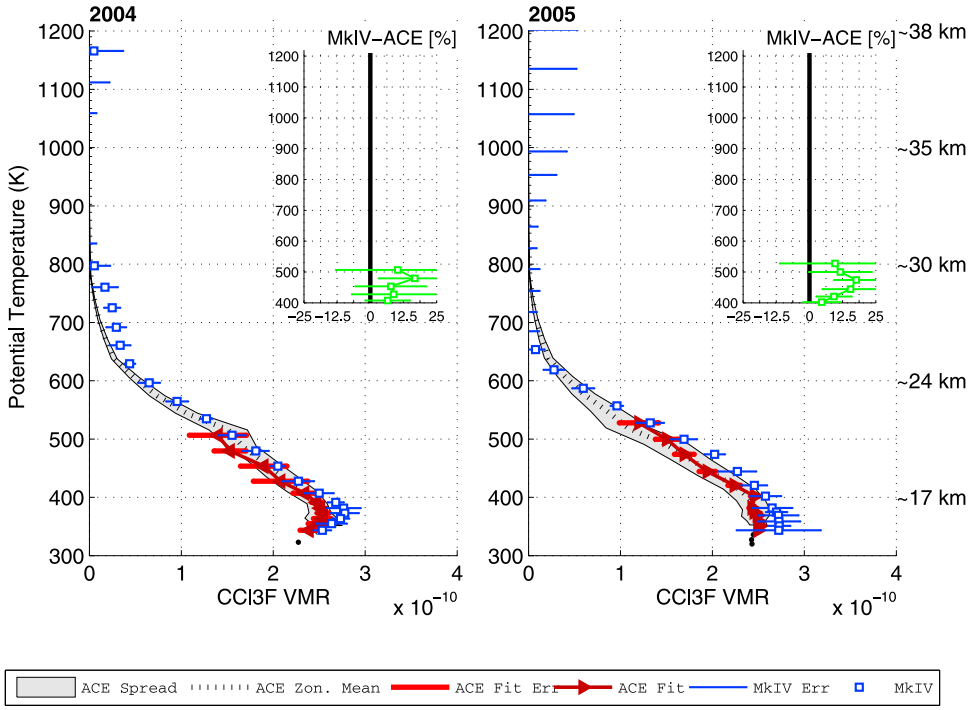

Figure 13. MkIV and ACE CCl_3F (CFC-11) comparisons. Details as for Figure 4.

10 years in the lower stratosphere below 30 km [*Kleinböhl et al.*, 2006]. This long lifetime means that the variability induced by HCN sources would still be observable in the upper troposphere and stratosphere. *Pumphrey et al.* [2008], observed a 2 year cycle of HCN in the stratosphere using MLS and ACE data. For our MkIV comparison, ACE data could be used up to 26 km. MkIV and ACE profiles both capture the same HCN structure (Figure 15). Considering

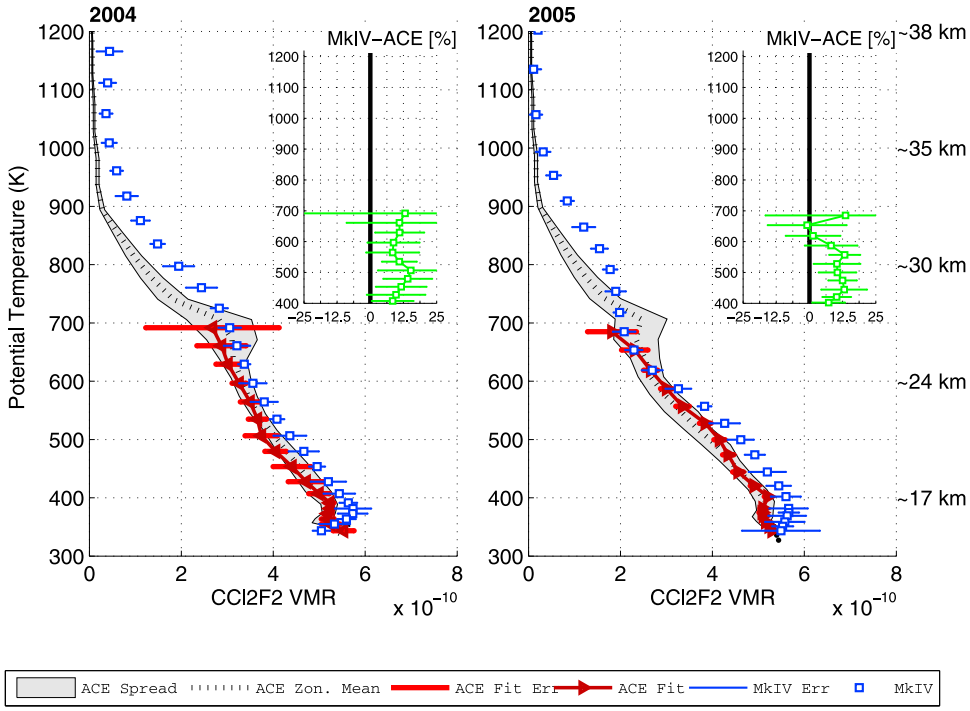

Figure 14. MkIV and ACE CCl_2F_2 (CFC-12) comparisons. Details as for Figure 4.

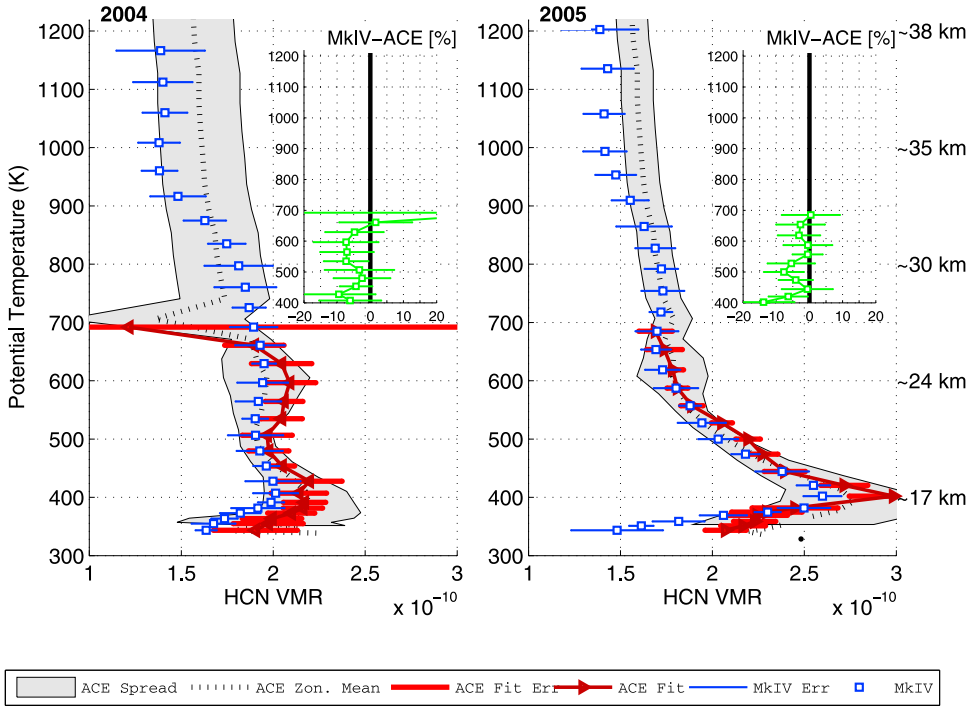

Figure 15. MkIV and ACE HCN comparisons. Details as for Figure 4.

the long lifetime of HCN, it is not surprising that both instruments would capture the same features of the profile. The profiles agree to within 15% from 400 K to about 650 K (~17 to 26 km), especially after using the recent updates to HITRAN according to *Kleinböhl et al.* [2006]. For 2004, the differences are mostly better than 10% from 400 K to 650 K. Differences become large above and below these altitudes.

3.8. CO

[31] CO is another trace gas that has its main source in the troposphere from direct anthropogenic and biomass burning

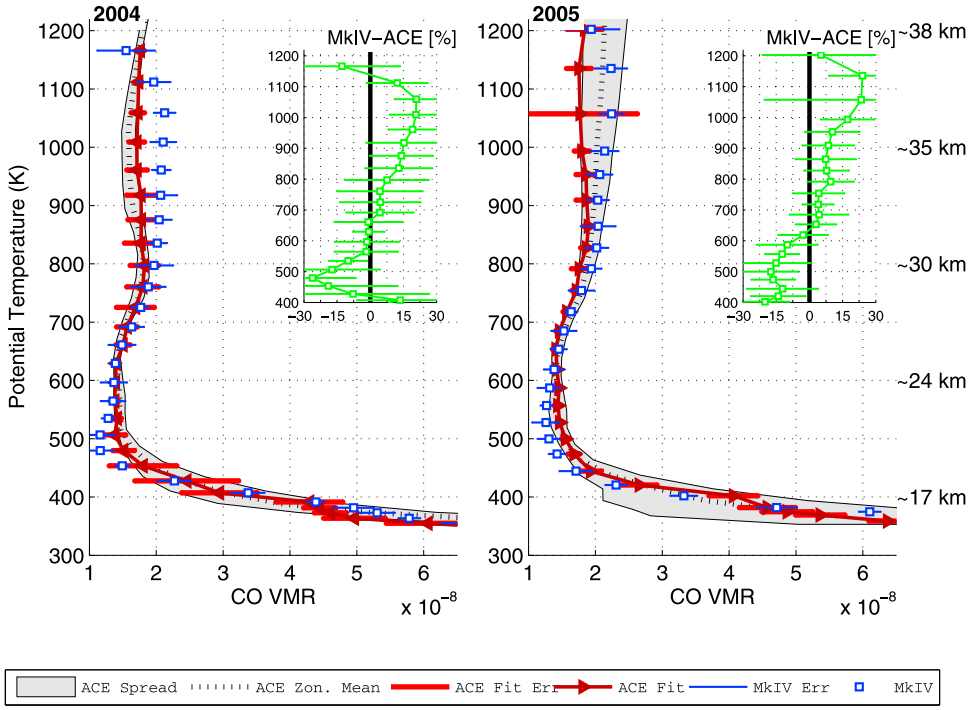

Figure 16. MkIV and ACE CO comparisons. Details as for Figure 4.

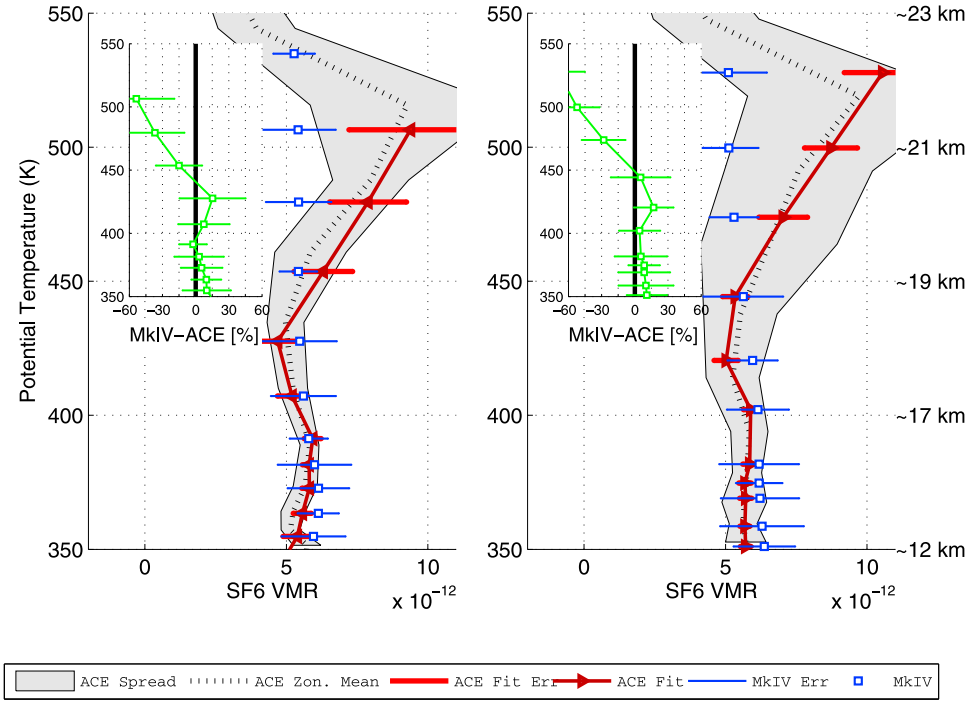

Figure 17. MkIV and ACE SF_6 comparisons. Details as for Figure 4.

emissions. It has a lifetime of a few weeks to months in the troposphere. Its main sink is its reaction with OH. In the stratosphere CO is produced from oxidation of hydrocarbons including methane. *Clerbaux et al.* [2008] used coincident measurements and reported an agreement of better than 22% (at 14 km to 20 km) between ACE and SPIRALE CO measurements in the Arctic. Here, we see about the same agreement below 24 km. Although there are differences in the CO profiles of ACE and MkIV (shown in Figure 16), they both capture the structure of the CO profile up to about 800 K (~30 km). Above 30 km ACE systematically measures less CO than MkIV (by up to 20% at 35 km altitude). Given the time difference between the MkIV and ACE measurements, these large discrepancies in the stratosphere may be in part due to seasonally dependent CO production in the stratosphere such as from CH_4 oxidation. Note that although all the MkIV EqL values fall within the ACE EqL values, the ACE measurements for 2004 were all taken after the MkIV flight and none before the MkIV flight, This explains the larger spread in the ACE data in the stratosphere for 2005 compared to 2004 (gray shaded area). *Velazco et al.* [2007, Figure 6] showed that at high latitudes, the summer-to-fall CO amount in the stratosphere can be dominated by the contribution from CH_4 oxidation at around 18–26 km and that this contribution can vary by ~7% from around July to around October.

3.9. SF_6, OCS, CF_4, CH_3Cl, and CHF_2Cl

[32] Sulfur hexafluoride (SF_6) is industrially produced and used as an insulating gas in high-voltage electrical and electronic equipment. SF_6 is the most potent greenhouse gas with a global warming potential of 22,800 times that of CO_2 when compared over a 100 year period [*Intergovernmental Panel on Climate Change*, 2007]. *Rinsland et al.* [2005] evaluated SF_6 trends from ACE and ATMOS measurements which indicated a continued rapid rise in the SF_6 lower stratospheric accumulation. Between 1985 and 1994, SF_6 increased by a factor (2.205 ± 0.211). Between 1985 and 2004 it increased by a factor (4.197 ± 0.394). These increases were found to be consistent with surface measurements. Figure 17 shows SF_6 VMRs measured from MkIV and compared with ACE. Figure 17 is limited to the 350 K to 550 K (12–23 km) altitude range for clarity. Using the method described here, both measurements agree well (within ±15%) from about 350 K to 450 K (~12–19 km) for both years. SF_6 above 18 km is very difficult to measure because of large errors arising from the weakness of the SF_6 absorption. The ACE SF6 increases with altitude exceeding 9 ppt by 21 km altitude. The MkIV profiles show a more constant profile, decreasing from about 6 ppt at 12 km to 5 ppt at 22 km. *Rinsland et al.* [1990] showed SF_6 errors ranging from 10% below 15 km to 40% above 20 km.

[33] OCS is considered to be a major source of stratospheric sulfate aerosol during periods of volcanic quiescence. *Notholt et al.* [2003] used MkIV OCS profiles, together with other data sets to study the impact of OCS on the stratospheric sulfate aerosol layer. Biomass burning is also an important source of OCS as reported by *Rinsland et al.* [2007] using ACE data. However, OCS profiles from MkIV and ACE have not been compared before. Here, we show comparisons of MkIV and ACE Carbonyl sulfide (OCS) profiles (Figure 18). Measurements indicate a ~15% bias at all altitudes with MkIV producing larger VMRs.

[34] Another potent greenhouse gas, carbon tetrafluoride (CF_4) has 7,390 times more greenhouse warming potential than CO_2 on a per molecule basis over a 100 year time horizon [*Intergovernmental Panel on Climate Change*,

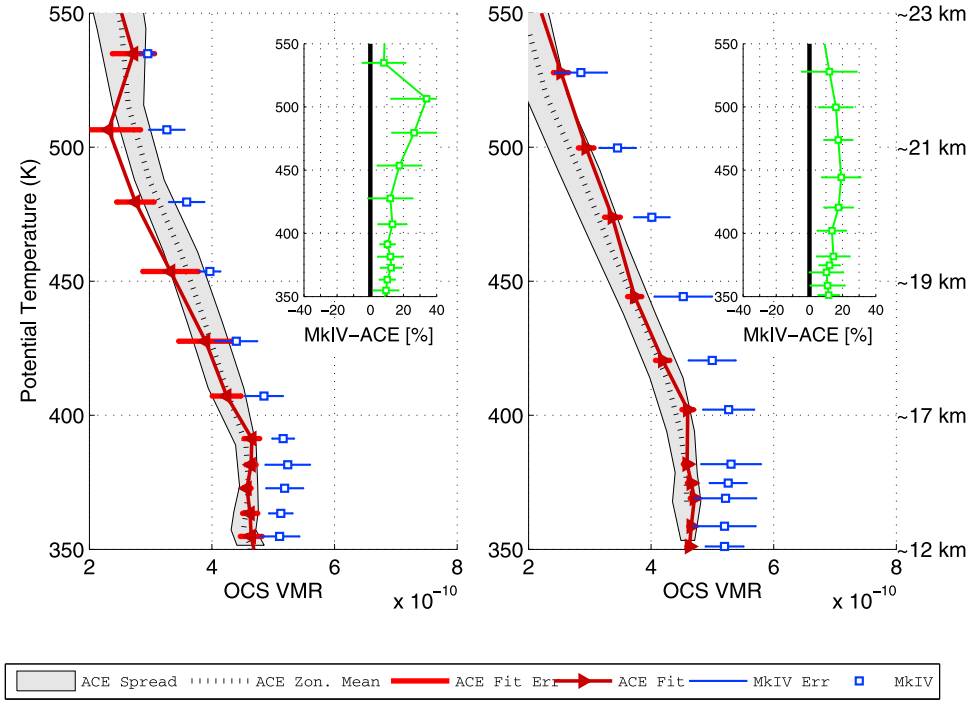

Figure 18. MkIV and ACE OCS comparisons. Details as for Figure 4.

2007]. Anthropogenic CF_4 emission is a byproduct of primary aluminum production. It has a very long atmospheric lifetime and has an increasing abundance in the atmosphere. Figure 19 shows MkIV and ACE CF_4 profiles. Measurements from both instruments agree well and are close to or within 10% above 500 K to 1200 K (see also Table 1).

[35] Methyl chloride (CH_3Cl) sources are believed to be located mostly in tropical and subtropical terrestrial regions

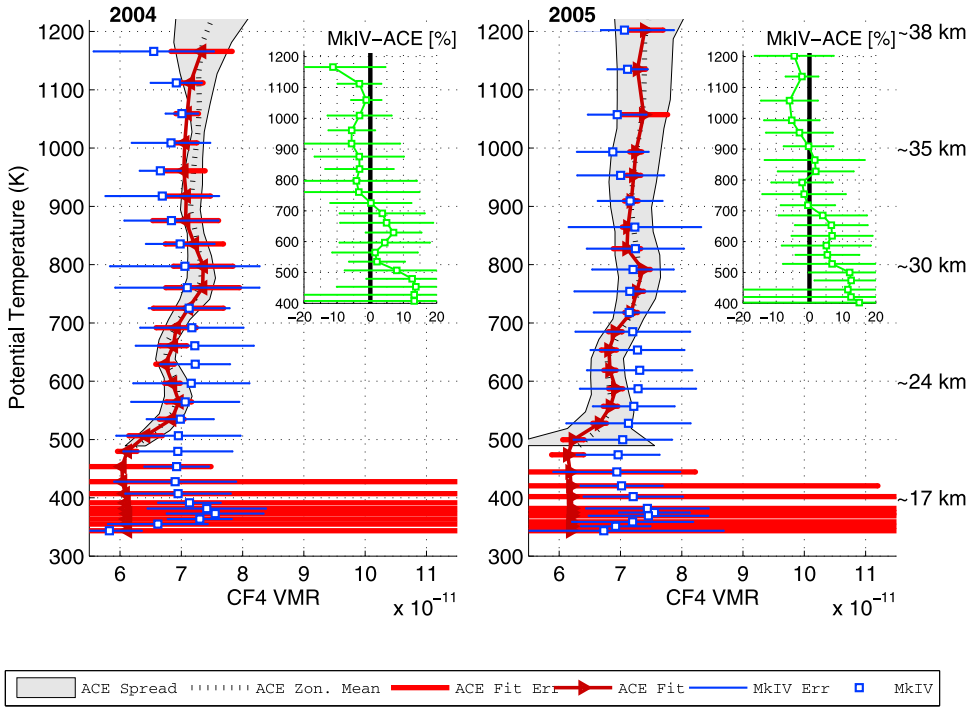

Figure 19. MkIV and ACE CF_4 comparisons. Details as for Figure 4.

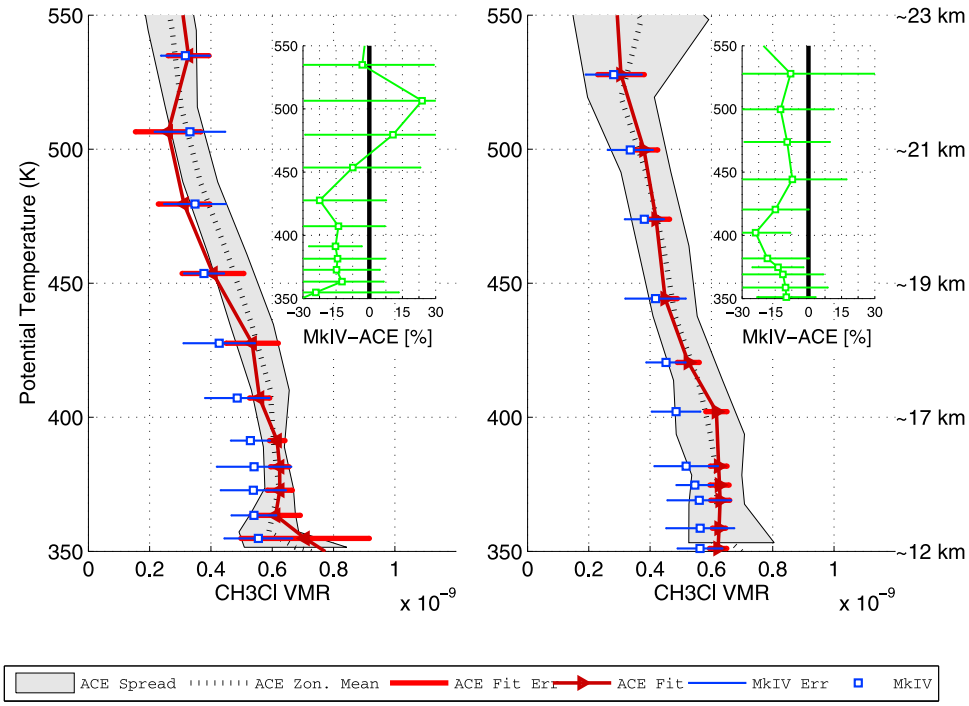

Figure 20. MkIV and ACE CH_3Cl comparisons. Details as for Figure 4.

with primary emissions from biomass burning, oceans, and the biosphere, however, large uncertainties remain in its budget [*World Meteorological Organization*, 2006]. Comparisons for this gas are shown in Figure 20. Differences between MkIV and ACE are within ±30%, with ACE measuring consistently more below 450 K for both years. We also show comparisons of CHF_2Cl (HCFC-22), a gas once used an alternative to CFC-11 and CFC-12 (Figure 21). MkIV–ACE measurements of HCFC-22 have differences within ±20% below 550 K. Above 600 K, no ACE data were used (very large errors or no measurements).

4. Summary and Conclusions

[36] ACE and MkIV profiles compare well using the method we have described, especially for long-lived gases. Because we take into account equivalent latitudes and potential temperature, this method of validation can meaningfully compare measurements of trace gas profiles that validation schemes using strict spatial and temporal coincidence criteria would reject. In the examples presented, the compared ACE and MkIV observations differed by more than six weeks and 180 deg of longitude and up to 10 degrees of latitude.

[37] Although ACE and MkIV are very similar instruments measuring in almost the same spectral regions, the microwindows used for the retrieval of profiles are different in some cases. This could lead to differences in the retrieved profiles if there are inconsistencies in the spectroscopic parameters. This could be the case for O_3 and OCS.

[38] An interesting feature present in both the ACE and MkIV data is a "fold" in the VMR profiles of the long-lived tracers at ~700 K. This is characterized by a reduction (or reversal) of the normal vertical VMR gradients. The fact that this feature appears in both MkIV and ACE data sets, and is present in both years (2004/2005) suggests that it is a robust feature at 35°N in September. Indeed, inspection of MkIV balloon profiles from earlier years (before the launch of ACE), shows this fold to be present most years. At this point in time, this feature is still unexplained.

[39] We also point out the likelihood of a vertical misregistration in the retrieved profiles. For gases that are decreasing with altitude, e.g., N_2O, there seems to be a tendency for the MkIV VMRs to be larger than those of ACE. Conversely, for gases whose VMR increases with altitude, such as HF, SF_6, HCl, COF_2, O_3 and HNO_3 below 600 K (~24 km altitude), the MkIV VMRs are generally smaller than those from ACE (see also Table 1). This is suggestive of errors in the altitudes (or potential temperatures) from one or both instruments. However, given the limited amount of data, it is not yet possible to precisely determine this error. For some gases (e.g., HF) this appears to be the main source of disagreement.

[40] Another potential cause of disagreement is the slightly different vertical resolution of the two instruments. For ACE, the vertical resolution is limited mainly by the external field of view which, projected onto the limb, subtends 3.5 km at the tropopause to 4.0 km in the upper stratosphere. The MkIV FOV is smaller (<2 km) and so the MkIV vertical resolution tends to be limited by the separation of successive tangent altitudes, which vary from <1 km immediately below the balloon to 3 km in the lower stratosphere. The net result of this is that, despite the limiting factors being different, the MkIV and ACE vertical resolutions are very similar (3–4 km). We have therefore ignored the small differences in averaging kernels during the comparison.

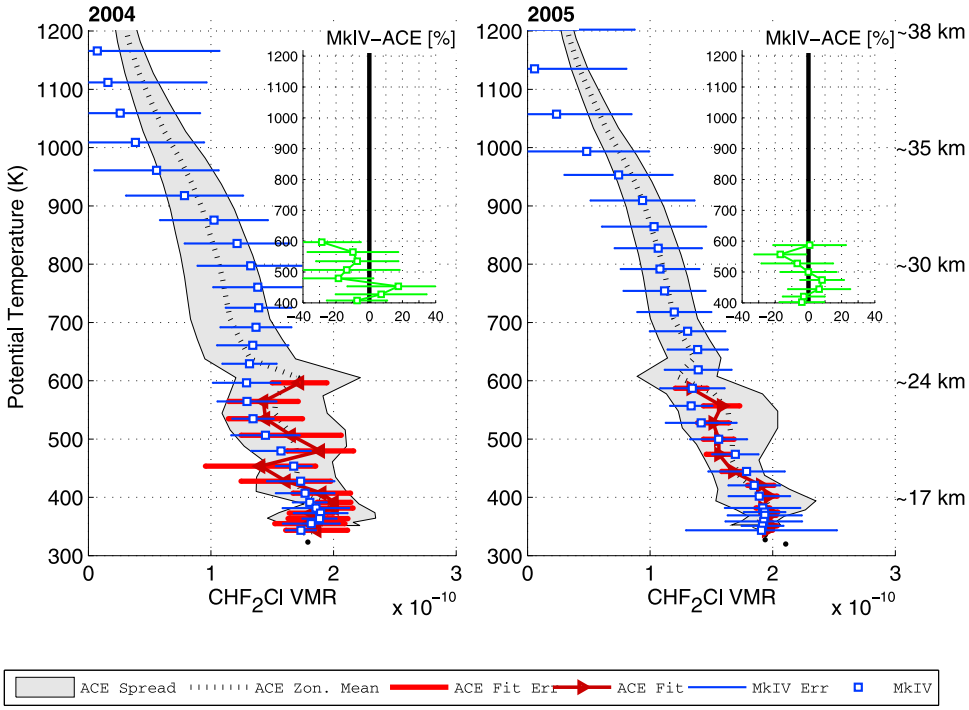

Figure 21. MkIV and ACE CHF_2Cl (HCFC-22) comparisons. Details as for Figure 4.

[41] Although the MkIV profiles do not satisfy the strict coincidence criteria for ACE validation, they are still very useful and they should be used, at least for long-lived gases whose VMR is conserved in a θ-*EqL* space. We have showed that despite the limited number of occultation measurements of the balloon-borne MkIV instrument, these high-precision measurements are still very much applicable for satellite validation with the help of derived meteorological products and a simple scheme to resample the satellite measurements in θ-EqL space to the location of the balloon observations. In this study, we therefore note the relevance of future balloon flights for satellite validation.

[42] **Acknowledgments.** We sincerely thank the three anonymous reviewers for their very constructive comments and suggestions to improve the manuscript. We thank the Columbia Scientific Ballooning Facility (CSBF), which performed the balloon launches of the MkIV instrument described in this work. Part of this research was conducted at the Jet Propulsion Laboratory, California Institute of Technology, under contract with NASA. The ACE mission is supported primarily by the Canadian Space Agency. Some support was also provided by the UK Natural Environment Research Council (NERC).

References

Bernath, P. F., et al. (2005), Atmospheric Chemistry Experiment (ACE): Mission overview, *Geophys. Res. Lett.*, *32*, L15S01, doi:10.1029/2005GL022386.

Boone, C. D., R. Nassar, K. A. Walker, Y. Rochon, S. D. McLeod, C. P. Rinsland, and P. F. Bernath (2005), Retrievals for the atmospheric chemistry experiment Fourier-transform spectrometer, *Appl. Opt.*, *44*(33), 7218–7231, doi:10.1364/AO.44.007218.

Carleer, M. R., et al. (2008), Validation of water vapour profiles from the Atmospheric Chemistry Experiment (ACE), *Atmos. Chem. Phys. Discuss.*, *8*, 4499–4559, doi:10.5194/acpd-8-4499-2008.

Clerbaux, C., et al. (2008), CO measurements from the ACE-FTS satellite instrument: Data analysis and validation using ground-based, airborne and spaceborne observations, *Atmos. Chem. Phys.*, *8*, 2569–2594, doi:10.5194/acp-8-2569-2008.

De Mazière, M., et al. (2008), Validation of ACE-FTS v2.2 methane profiles from the upper troposphere to the lower mesosphere, *Atmos. Chem. Phys.*, *8*, 2421–2435, doi:10.5194/acp-8-2421-2008.

Dupuy, E., et al. (2009), Validation of ozone measurements from the Atmospheric Chemistry Experiment (ACE), *Atmos. Chem. Phys.*, *8*, 287–343, doi:10.5194/acp-9-287-2009.

Farmer, C. B. (1987), High resolution infrared spectroscopy of the Sun and the earth's atmosphere from space, *Mikrochim. Acta*, *III*, 189–214.

Froidevaux, L., et al. (2006), Early validation analyses of atmospheric profiles from EOS MLS on the Aura satellite, *IEEE Trans. Geosci. Remote Sens.*, *44*, 1106–1121, doi:10.1109/TGRS.2006.864366.

Hegglin, M. I., C. D. Boone, G. L. Manney, T. G. Shepherd, K. A. Walker, P. F. Bernath, W. H. Daffer, P. Hoor, and C. Schiller (2008), Validation of ACE-FTS satellite data in the upper troposphere/lower stratosphere (UTLS) using non-coincident measurements, *Atmos. Chem. Phys.*, *8*, 1483–1499, doi:10.5194/acp-8-1483-2008.

Intergovernmental Panel on Climate Change (2007), Direct global warming potentials, in *Climate Change 2007: The Physical Science Basis. Contribution of Working Group I to the Fourth Assessment Report of the Intergovernmental Panel on Climate Change*, chap. 2.10.2, Cambridge Univ. Press, Cambridge, U. K.

Irie, H., et al. (2006), Validation of stratospheric nitric acid profiles observed by Improved Limb Atmospheric Spectrometer (ILAS)-II, *J. Geophys. Res.*, *111*, D11S03, doi:10.1029/2005JD006115.

Kleinböhl, A., G. C. Toon, B. Sen, J. L. Blavier, D. K. Weisenstein, R. S. Strekowski, J. M. Nicovich, P. H. Wine, and P. O. Wennberg (2006), On the stratospheric chemistry of hydrogen cyanide, *Geophys. Res. Lett.*, *33*, L11806, doi:10.1029/2006GL026015.

Lait, L. R., et al. (2004), Non-coincident inter-instrument comparisons of ozone measurements using quasi-conservative coordinates, *Atmos. Chem. Phys.*, *4*, 2345–2352, doi:10.5194/acp-4-2345-2004.

Mahieu, E., et al. (2008), Validation of ACE-FTS v2.2 measurements of HCl, HF, CCl_3F and CCl_2F_2 using space-, balloon- and ground-based instrument observations, *Atmos. Chem. Phys.*, *8*, 6199–6221, doi:10.5194/acp-8-6199-2008.

Manney, G. L., et al. (2001), Comparison of satellite ozone observations in coincident air masses in early November 1994, *J. Geophys. Res.*, *106*(D9), 9923–9943, doi:10.1029/2000JD900826.

Manney, G. L., et al. (2007), Solar occultation satellite data and derived meteorological products: Sampling issues and comparisons with Aura

Microwave Limb Sounder, *J. Geophys. Res.*, *112*, D24S50, doi:10.1029/2007JD008709.

Minschwaner, K., et al. (2010), The photochemistry of carbon monoxide in the stratosphere and mesosphere evaluated from observations by the Microwave Limb Sounder on the Aura satellite, *J. Geophys. Res.*, *115*, D13303, doi:10.1029/2009JD012654.

Moreau, G., C. Robert, V. Catoire, M. Chartier, C. Camy-Peyret, N. Huret, M. Pirre, L. Pomathiod, and G. Chalumeau (2005), SPIRALE: A multi-species in situ balloon-borne instrument with six tunable diode laser spectrometers, *Appl. Opt.*, *44*(28), 5972–5989, doi:10.1364/AO.44.005972.

Nakajima, H., et al. (2006), Measurements of ClONO2 by the Improved Limb Atmospheric Spectrometer (ILAS) in high-latitude stratosphere: New products using version 6.1 data processing algorithm, *J. Geophys. Res.*, *111*, D11S09, doi:10.1029/2005JD006441.

Notholt, J., et al. (2003), Enhanced upper tropical tropospheric COS: Impact on the stratospheric aerosol layer, *Science*, *300*, 307–310, doi:10.1126/science.1080320.

Notholt, J., G. C. Toon, S. Fueglistaler, P. O. Wennberg, F. W. Irion, M. McCarthy, M. Scharringhausen, T. Siek Rhee, A. Kleinböhl, and V. Velazco (2010), Trend in ice moistening the stratosphere–constraints from isotope data of water and methane, *Atmos. Chem. Phys.*, *10*, 201–207, doi:10.5194/acp-10-201-2010.

Pumphrey, H. C., C. Boone, K. A. Walker, P. Bernath, and N. J. Livesey (2008), The tropical tape recorder observed in HCN, *Geophys. Res. Lett.*, *35*, L05801, doi:10.1029/2007GL032137.

Randall, C. E., et al. (2002), Validation of POAM III NO_2, *J. Geophys. Res.*, *107*(D20), 4432, doi:10.1029/2001JD001520.

Rinsland, C. P., A. Goldman, F. Murcray, R. D. Blatherwick, J. J. Kosters, D. G. Murcray, N. D. Sze, and T. Massie (1990), Long-term trends in the concentrations of SF_6, $CHClF_2$ and COF_2 in the lower stratosphere from analysis of high-resolution infrared solar occultation spectra, *J. Geophys. Res.*, *95*(D10), 16,477–16,490, doi:10.1029/JD095iD10p16477.

Rinsland, C. P., R. J. Salawitch, G. B. Osterman, F. W. Irion, B. Sen, R. Zander, E. Mahieu, and R. Gunson (2000), Stratospheric CO at tropical and midlatitudes: ATMOS measurements and photochemical steady state model calculations, *Geophys. Res. Lett.*, *27*(9), 1395–1398, doi:10.1029/1999GL011184.

Rinsland, C. P., C. Boone, R. Nassar, K. Walker, P. Bernath, E. Mahieu, R. Zander, J. C. McConnell, and L. Chiou (2005), Trends of HF, HCl, CCl_2F_2, CCl_3F, $CHClF_2$(HCFC-22), and SF_6 in the lower stratosphere from Atmospheric Chemistry Experiment (ACE) and Atmospheric Trace Molecule Spectroscopy (ATMOS) measurements near 30°N latitude, *Geophys. Res. Lett.*, *32*, L16S03, doi:10.1029/2005GL022415.

Rinsland, C. P., G. Dufour, C. D. Boone, P. F. Bernath, L. Chiou, P.-F. Coheur, S. Turquety, and C. Clerbaux (2007), Satellite boreal measurements over Alaska and Canada during June–July 2004: Simultaneous measurements of upper tropospheric CO, C_2H_6, HCN, CH_3Cl, CH_4, CH_3OH, HCOOH, OCS, and SF_6 mixing ratios, *Global Biogeochem. Cycles*, *21*, GB3008, doi:10.1029/2006GB002795.

Russell, J. M., III, et al. (1996), Validation of hydrogen fluoride measurements made by the Halogen Occultation Experiment from the UARS platform, *J. Geophys. Res.*, *101*(D6), 10,163–10,174, doi:10.1029/95JD01705.

Sen, B., G. C. Toon, J.-F. Blavier, E. L. Fleming, and C. H. Jackman (1996), Balloon-borne observations of mid-latitude fluorine abundance, *J. Geophys. Res.*, *101*(D4), 9045–9054, doi:10.1029/96JD00227.

Steinwagner, J., S. Fueglistaler, G. Stiller, T. von Clarmann, M. Kiefer, P. Borsboom, A. van Delden, and T. Röckmann (2010), Tropical dehydration processes constrained by the seasonality of stratospheric deuterated water, *Nat. Geosci.*, *3*, 262–266, doi:10.1038/ngeo822.

Strong, K., et al. (2008), Validation of ACE-FTS N_2O measurements, *Atmos. Chem. Phys.*, *8*, 4759–4786, doi:10.5194/acpd-8-3597-2008.

Toon, G. C. (1991), The JPL MkIV Interferometer, *Opt. Photon. News*, *2*, 19–21, doi:10.1364/OPN.2.10.000019.

Toon, G. C., et al. (1999), Comparison of MkIV balloon and ER-2 aircraft profiles of atmospheric trace gases, *J. Geophys. Res.*, *104*(D21), 26,779–26,790, doi:10.1029/1999JD900379.

Velazco, V., et al. (2007), Annual variation of strato-mesospheric carbon monoxide measured by ground-based Fourier transform infrared spectrometry, *Atmos. Chem. Phys.*, *7*, 1305–1312, doi:10.5194/acp-7-1305-2007.

Walker, K. A., C. E. Randall, C. R. Trepte, C. D. Boone, and P. F. Bernath (2005), Initial validation comparisons for the Atmospheric Chemistry Experiment (ACE-FTS), *Geophys. Res. Lett.*, *32*, L16S04, doi:10.1029/2005GL022388.

Wolff, M. A., et al. (2008), Validation of HNO_3, $ClONO_2$, and N_2O_5 from the Atmospheric Chemistry Experiment Fourier Transform Spectrometer (ACE-FTS), *Atmos. Chem. Phys.*, *8*, 3529–3562, doi:10.5194/acp-8-3529-2008.

World Meteorological Organization (2006), Controlled substances and other source gases, in Scientific Assessment of Ozone Depletion: 2006, *Rep. 50*, pp. 1.1–1.83, Global Ozone Res. and Monit. Proj., Geneva, Switzerland.

Wunch, D., M. P. Tingley, T. G. Shepherd, J. R. Drummond, G. W. K. Moore, and K. Strong (2005), Climatology and predictability of the late summer stratospheric zonal wind turnaround over Vanscoy, Saskatchewan, *Atmos. Ocean*, *43*(4), 301–313, doi:10.3137/ao.430402.

P. F. Bernath, Department of Chemistry, University of York, Heslington, York YO10 5DD, UK.

J.-F. L. Blavier, W. H. Daffer, A. Kleinböhl, G. L. Manney, and G. C. Toon, Jet Propulsion Laboratory, California Institute of Technology, 4800 Oak Grove Dr., Pasadena, CA 91109, USA.

C. Boone, Department of Chemistry, University of Waterloo, Waterloo, ONT, Canada N2L 3G1.

V. A. Velazco, Institute of Environmental Physics, University of Bremen, Otto-Hahn-Allee 1, D-28359 Bremen, Germany. (voltaire@iup.physik.uni-bremen.de)

K. A. Walker, Department of Physics, University of Toronto, 60 St. George St., Toronto, ONT, Canada M5S 1A7.